Return to previous file: MCU10.pdf

Figure 8 shows that the model is reproducing the basic alongshore flow features reasonably well. There are periods when the modelled alongshore flows are offset from those measured, particularly from 14-23 September. These offsets are related to low-frequency oscillations in the measured data, probably associated with large-scale weather-related flow events, such as coastal-trapped waves that are not represented in the model. The model does reasonably well considering the absence of any large-scale forcing, and also that the input winds were from a land-based weather station that is likely to be a poor substitute for ocean winds (e.g.. Hsu 1986, Laing et al. 1997). Figure 9 shows that the cumulative flow vector has a similar order of magnitude, which suggests that a floating larva would travel about the right distance. Based on this calibration we are confident that the model performs satisfactorily when forced by alongshore tidal fluxes, winds measured at Gisborne Airport and appropriate wave radiation stresses.

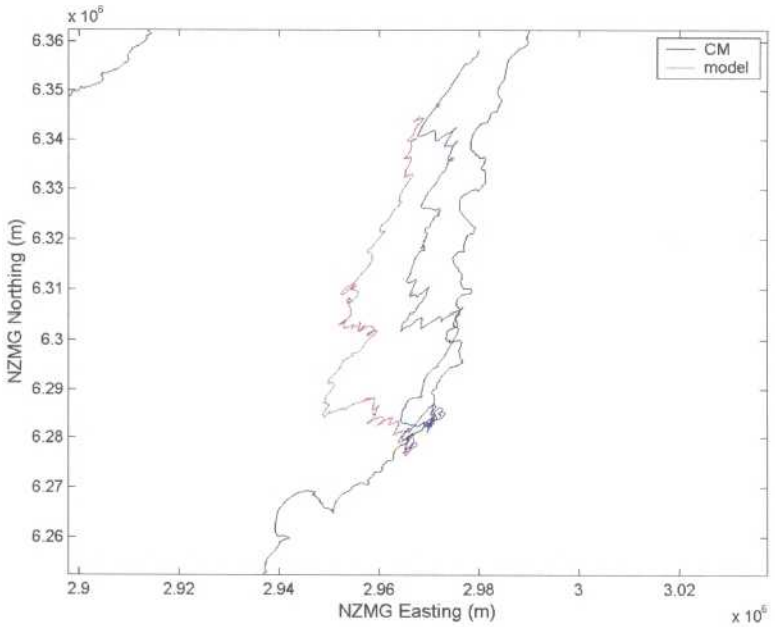

Figure 9. Cumulative vector plot of measured and calibrated model currents, using an open boundary flux based on the tidal component of the measured alongshore current, wind measured at Gisborne Airport and mean wave conditions during the deployment.

It was not possible to achieve a reasonable calibration at the inshore current-meter site, because there were processes occurring at the inshore site that are not reproducible by the hydrodynamic model. The inshore site is characterised by strong and variable cross-shore flows that are caused by wave-driven currents buffeting around in the

complex rocky-reef habitat. The hydrodynamic model included a stationary wave forcing component, but could not represent the variable nature of these surfzone currents. Figure 10 illustrates the highly variable and rapidly fluctuating nature of the currents at the inshore current-meter site. The cross-shore currents in particular were larger and more variable than at the offshore site (c.f. Figure 8). The largest cross-shore currents are seen to have occurred when the waves were biggest, e.g. 6-13 and 22-25 September, and 6 October.

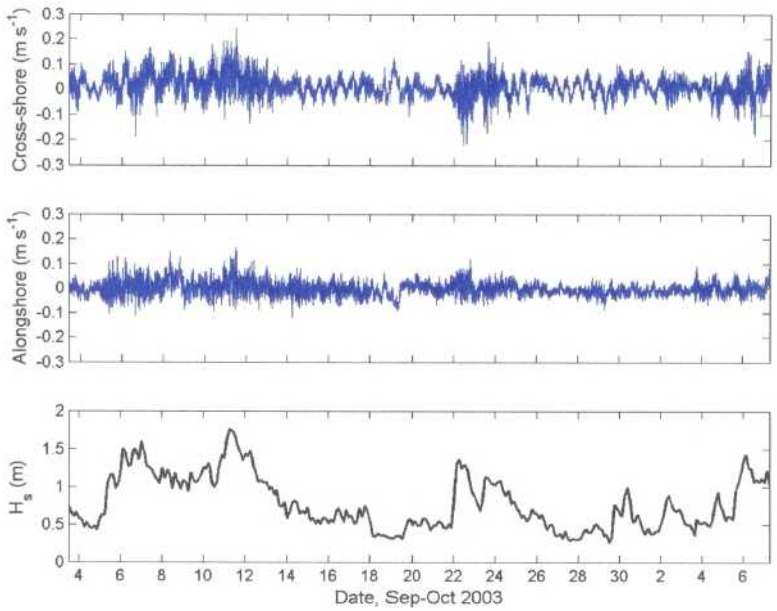

Figure 10. Cross-shore and alongshore currents (depth-averaged 2-8 m) and significant wave heights measured at the inshore current-meter site.

4. Larval dispersal methods

4.1 Hydrodynamic scenarios

Having obtained a reasonable calibration, the hydrodynamic model was then used to simulate a range of scenarios during which larval dispersal might occur, comprising average, calm and two storm conditions (Table 3). The open boundaries for all scenario simulations were forced by tidal fluxes comprising the K_1, O_1 and M_2 tidal components that make up the majority of the tidal signal in this area. The first of these scenarios attempted to represent the long-term mean conditions experienced on this part of the coast, combining the tidal forcing with long-term average wind and wave conditions. A 10-year wind record from Gisborne Airport was obtained, and the scalar-average speed and vector-average direction were found to be 3.5 m s^{-1} from 315° respectively. The average significant wave height, wave propagation direction and mean-period obtained from the 20-year wave hindcast were 1.7 m, 205° and 7.0 s respectively. A calm scenario was simulated without wind or waves, along with scenarios of strong wind and wave action with approach directions from the S and E, which might be expected to create the maximum along-coast dispersal to the northeast and southwest respectively (Table 3). The scenarios were simulated for the time period 3-30 September 2003.

Table 3. List of conditions making up the 4 hydrodynamic scenarios for which larval dispersal was simulated. Winds and wave direction are meteorological convention (coming from).

#	Scenario	Tides	Wind	Waves	Scenario
1	Calm	K_1, O_1, M_2	None	None	Calm
2	Average	K_1, O_1, M_2	Average: 3.5 m s^{-1} from 315°	H_s = 1.7 m, D = 205°, T_m = 7.0 s	Average
3	Southerly storm	K_1, O_1, M_2	22 Jan–23 Feb 1996, average 3.8 m s^{-1} from 225°	H_s = 2.1 m, D = 188°, T_m = 6.9 s	Southerly storm
4	Easterly storm	K_1, O_1, M_2	4 Dec 1988–4 Jan 1989, average 4.9 m s^{-1} from 31°	H_s = 2.0 m, D = 86°, T_m = 6.8 s	Easterly storm

To force the strong-wind scenarios, time periods of actual winds from the historical Gisborne Airport record were examined, to find periods where the average wind strength along the approach axis was close to the 99th percentile. The selected time periods were from 22 Jan-23 Feb 1996 and 4 Dec 1988-4 Jan 1989 for approach axes 180° and 90° respectively. The associated wave forcing fields were obtained by

finding all waves in the 20-year hindcast approaching from 22.5° either side of the approach axis, then taking the average of the storm waves amongst these, storm waves being selected using a peaks-over-threshold method with a 2-day threshold.

4.2 Particle-analysis methods

The following bullet-points describe terms that refer to stages or processes involved in larval dispersal, settlement and recruitment.

- Larvae are released from existing adult populations.
- *Larval supply* to the adjacent coast is a product of the adult population size x fecundity, and advection of larvae *(dispersal)* in the currents.
- *Settlement potential* is related to the "competency" of larvae on encountering suitable habitat, for example paua larvae don't become competent to settle for at least 3 days. If they settle before they are "competent", or in depths outside their habitat range they won't survive.
- *Recruitment* of larvae is a function of settlement and post-settlement survival. If larvae settle on unsuitable substrates, they will perish.

The output from this study are maps of *larval supply*. The larval settlement distribution does not necessarily match the adult population distribution, because *settlement potential* and *recruitment* must also be accounted for. We have attempted to incorporate depth-related *settlement potential* into the *larval supply* maps, but leave it to the reader to infer *recruitment* based on their knowledge of (1) the types of habitat that are suitable, and (2) the locations of those habitat types. No attempt has been made to categorise or map substrate type on which larvae settle, so the result plots in the next section need to be interpreted as such.

Twenty larval dispersal simulations were undertaken, for all combinations of the five larvae and spore types (kelp, kina, limpets, paua, pupu) and the four hydrodynamic simulations (Table 3). In the model, larvae and spores are treated identically and in this report are simply referred to as larvae. For each species, larvae were released at source points corresponding to the locations supplied in Table 4, i.e. each species had multiple release locations. Larval durations were set to the maximum of the range for each species (Table 4), to identify their maximum dispersion range.

Larvae were released instantaneously at the beginning of each simulation, and thereafter every 2.7 days, with the fifth and last release occurring after 13.5 days (Figure 11). Therefore all species have the same number and timing of releases, which simplifies the comparison of simulated larval dispersal patterns between species.

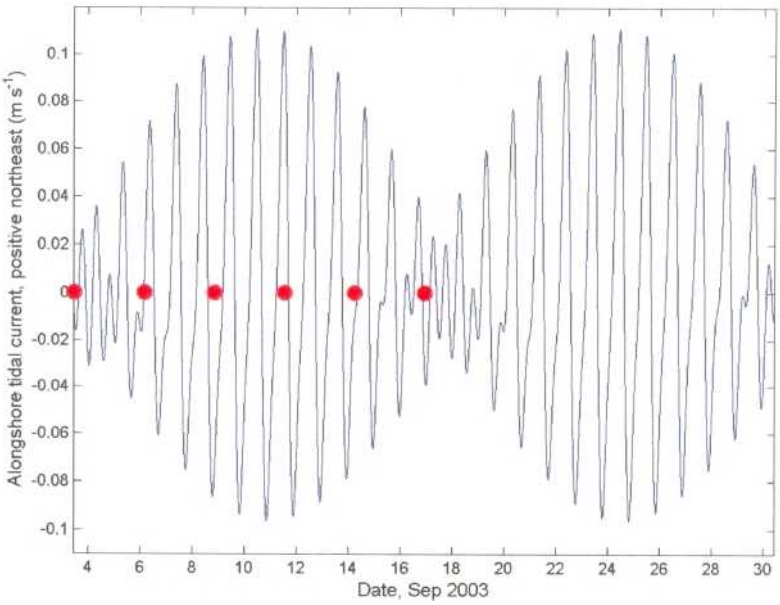

Figure 11. Alongshore tidal current speed used to force the 4 hydrodynamic scenarios for dispersal modelling (Table 3). The red dots mark the larval release times.

In reality, the total number of larvae released will be the product of the adult reproductive population size x fecundity. Fecundity varies between species, and is likely to be inversely related to larval duration and directly related to larval mortality (e.g. Vance 1973; Christiansen and Ferchel 1979). The production of fewer, larger eggs by some species (with the provision of more yolk from the mother) means that the resultant larvae are further developed upon hatching and are soon competent to settle (i.e. a short larval duration). In contrast, other species produce vast quantities of tiny eggs, but the resultant larvae require long periods of time in the water column for feeding and development until competency. It was not possible to model the variability introduced by these relationships because adult population size and rates of larval mortality in the water column are not well characterised. In particular, we don't know enough to make reasonable estimates of larval mortality. The role of mortality is assumed by the use of the 1st-order sedimentation method (Section 2.5), whereby

larvae are removed from the simulation when they encounter the seabed. If their first point of contact is offshore and deeper than where they normally occur, they are considered "lost" from our model system (It is assumed that they died). The animal species being simulated are broadcast spawners, whose strategy for reproduction is to produce massive numbers of eggs, sperm, or larvae, with the aim of having a tiny fraction survive to adulthood. Some particles never do encounter the seabed within the specified larval duration, and these are also assumed lost by the model, as they failed to reach suitable habitat.

The settling rate of the larvae is an important control on their dispersal pattern. Paua are thought to have a sinking rate of 20 mm s^{-1} when not actively swimming upward, and bull kelp spores sink at a rate of 0.36 mm s^{-1} (Taylor et al. 2004). There was no information available for the other species, therefore a default sinking rate of lx 10^{-4} m s^{-1} was applied, about 10 m per 24 hours. With paua larvae being able to swim, their averaging sinking speed is unknown, so the default speed of lx 10^{-4} m s^{-1} was used. Using the non-swimming sinking speed of paua allowed for almost no dispersion, they all settled very close to their release site.

Although the larvae in our model may contact the seabed in any depth, they will only recruit successfully if they settle at a depth conducive to their survival. For the 3 intertidal species, (bull kelp, limpets and pupu) larvae have only been counted if they settled in depths less than 2 m relative to low tide. Kina were counted at all depths, and paua were counted both at all depths and again at depths < 5 m relative to low tide (Section 5, Appendix 1).

Fecundity was not known for all species. We have used a nominal fecundity of 50,000 larvae per release, for all species. This does not affect the simulation results, because larvae are represented as a sediment concentration by the model (Section 2.5). It has a minor effect in the interpretation of the results via equation l, when the concentrations are converted to larvae numbers and rounded to the nearest whole larvae, before converting to percentages for presentation (Section 5). However, the errors associated with using the constant fecundity are probably small compared with the unknown total larvae release number and mortality, and justified because of the clarity added to inter-species comparisons.

Table 4. Details of larval release locations, fecundity and duration for the target species. All data were supplied by the Department of Conservation, except for the last 2 columns that specify simulation details.

Common name	Species	Easting (NZMG)	Northing (NZMG	Larval duration (days)
	Turbo			4
pupu, cat's eye	*smaragdus*	2962487	6275260	
		2962920	6276692	
	Melagraphia			
pupu, topshell	*aethiops*	2962380	6275438	
pupu, Cook's turban	*Cookia sulcata*	2963035	6275462	
ngakihi, limpets	*Cellana spp*	2962920	6276692	2-10
		2962487	6275260	
bull kelp	*Durvillaea*	2963229	6275137	0.25-0.5
		2962352	6275168	
		2962925	6275145	
		2965202	6278351	
black foot paua	*Haliotis iris*	2962487	6275260	3--11
		2962920	6276692	
		2965202	6278351	
		2963035	6275462	
		2962352	6275168	
	Evechinus			20-30
kina	*chloroticus*	2962570	6275337	
		2962352	6275168	

5. Larval dispersal results and discussion

The principle of a marine reserve is to allow adult spawning populations to build up in absence of harvesting pressure. If adult populations increase in the marine reserve, then *larval supply* will increase in tandem, and these simulation results show the likely range of supply to the nearby coast.

The output of the larval dispersal simulations is displayed as a series of shaded density plots in Appendix 1. An example is shown in Figure 10. The larval density has been displayed as a percentage of the total number of larvae released from a single point source during the simulation, point sources are marked (*). The following results are evident from the plots in Appendix 1.

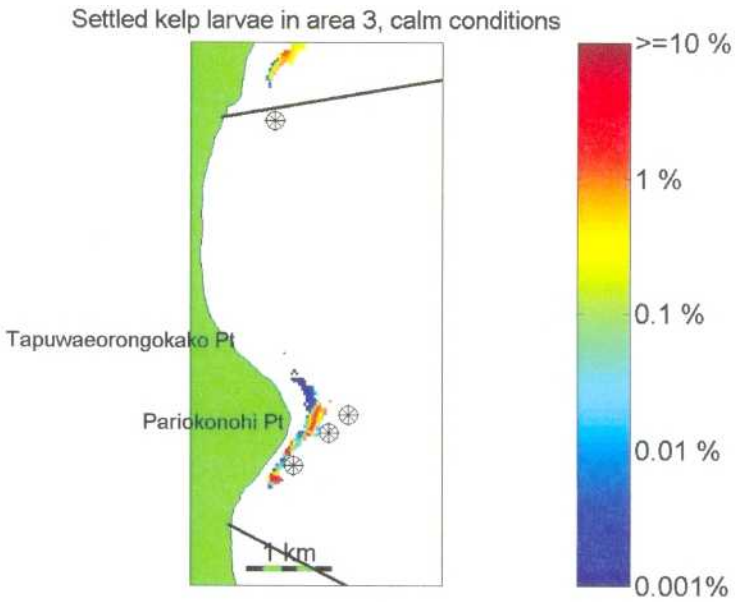

Figure 10. Shaded density plot of the settled percentage of bull kelp larvae in Area 3 (e.g. Figure 2), released during calm-weather (hydrodynamic scenario 1, Table 3). The percentage values relate to the total number of larvae spawned at a single source point during the simulation. Particle release source points are marked (*). Settled larval percentages are only displayed for depths $\leq$ 2 m relative to low tide. Black lines mark the marine reserve boundary.

Larval dispersal was smallest during calm weather (HD scenario 1, Table 3), when currents were forced only by tides. The tidal currents oscillate back and forth along the

coast, with a maximum excursion distance of about 12 km, but typical excursion distance of about 3 km. Therefore the larvae tended to oscillate around their point of release and settled within about 2 km regardless of species. The direction of dispersal by tides tended towards the northeast, due to asymmetry of the tidal flow field over the local bathymetry.

The mean wind and wave conditions caused a northeast-directed alongshore current that carried larvae towards the northeast. Storm conditions from the south caused the widest dispersal of larvae, also pushing them to the northeast. Storm conditions from the east caused larvae to disperse away from their release point towards the southwest.

The longer the larval duration (Table 4), the greater the potential for larval dispersal, because dispersal is a product of current velocities and the amount of time spent floating in these currents. Therefore kina dispersed furthest, followed by paua, and bull kelp was least dispersive. Kina dispersed further north of Gable End Foreland and south to Tuaheni Point.

The other major control on dispersal is the sinking rate of the larvae after release. We have confidence in our estimates of bull kelp sinking rate, but the larval sinking rate of the other target species are not well known. Experimental work on larvae settling behaviour has the potential to considerably improve future dispersal modelling estimates.

Our results suggest that there is little export of bull kelp spores from adult populations in the marine reserve to rocky headlands outside the reserve. Only during easterly storm conditions did they settle on a headland outside the reserve area, making it south to Turihaua Point. This indicates that local bull kelp populations may be reproductively isolated, and localised population declines would not recover quickly via inputs from external sources.

Pupu and limpets recruit to the intertidal zone and model results suggest similar dispersal characteristics, reaching Gable End Foreland during average conditions and again in slightly higher numbers in the southerly storm. During the easterly storm they reached as far south as Tatapouri Point, with pupu settling there in higher numbers. This occurred because there were more release sites for pupu, with two release sites located on the southern side of Pariokonohi Point, whereas limpet larvae tended to be deflected offshore by Pariokonohi Point (the effect of headlands in deflecting current flows is explained further in the last paragraph).

Paua dispersed northward to Gable End Foreland during average conditions, and even further north during the southerly storm. During the easterly storm, paua dispersed to

just south of Tatapouri Point. We initially considered paua to recruit successfully at depths $\leq$ 5 m, but have also included plots for the situation where they could recruit at any depth shallower than 30 m. This effectively opens up a significantly larger habitat zone for the surviving larvae, allowing them to populate a much wider area, further from the spawning site. The plots in Figure 11 have been selected to demonstrate this effect. This demonstrates how habitat mapping could be used to enhance the accuracy of presentation of larval dispersal modelling, if available.

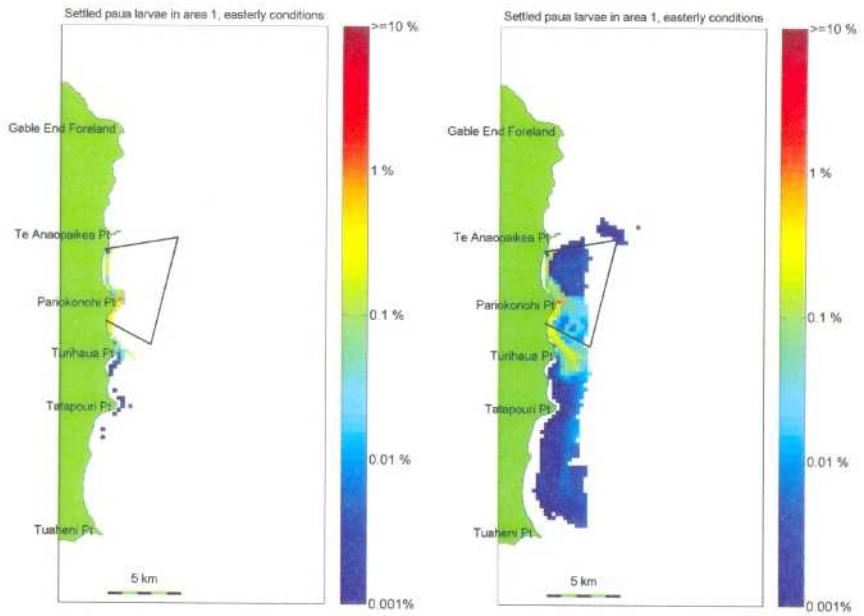

Figure 11. Shaded density plot of the settled percentage of paua larvae in Area 1, released during easterly storm conditions (hydrodynamic scenario 4, Table 3). The percentage values relate to the total number of larvae spawned at a single source point during the simulation. The left-hand plot displays settled larval percentages for depths $\leq$ 5m relative to low tide, while the right-hand plot shows for depths $\leq$ 30 m.

Species with spawning populations located on the Hinematikotai Rocks were more successful in dispersing northward past Whangara Island. The headlands provide barriers to currents flowing in the alongshore direction, deflecting them offshore and creating eddies in their lee, with Whangara Island being particularly effective. This tends to disrupt the alongshore migration of larvae caught up in the currents. As a consequence, Whangara Island provided a major barrier to northward dispersal of larvae from the reserve, and therefore trapped and accumulated larvae on its southern side at a relatively high rate. Therefore the most likely settling point for all larval types spawned at Pariokonohi Point is on the southern side of Te Anaopaikea Point and Whangara Island, where the adjacent shallow areas are the first point of interception

with habitable substrate for larvae drifting northward in the long-term average currents (assuming that there is no suitable substrate in the sandy bay separating the points).

The hydrodynamic model used for this study was 2-dimensional (depth-averaged), chosen for its ability to incorporate wave radiation stresses that are dominant in shallow nearshore areas where the target species are found (Section 2.4). The use of a 2D model means that flow variations in the vertical are lost. The primary cause for vertical flow variations away from large riverine inputs is from wind stress on the water surface. Although the general flow was approximately correct as shown by the model calibration, subtleties of the wind-driven flow were lost. Thus there are other levels of modelling complexity that have not been attempted here, which would particularly affect larvae that have the ability to control their vertical position in the water column, e.g. paua. To account for these 3D subtleties in future requires

1. implementation of a 3d model that incorporates wind stress and stratification, and

2. more research into the behaviour of larvae, and the fitting of this realistic larval behaviour into the particle-transport model.

6. References

Booij, N.; Ris, R.C.; Holthuijsen, L.H. (1999). A third-generation wave model for coastal regions, Part I, Model description and validation. *Journal of Geophysical Research 104(C4):* 7649-7666.

Christiansen, F.B.; Ferchel, T. M. (1979). Evolution of marine invertebrate reproductive patterns. *Theoretical Population Biology 16:* 267-282.

DHI Water and Environment (2003). MIKE21 and MIKE3 particle analysis and oil spill analysis user guide. 106 p.

Green, M.O.; Stroud, M.J.; Oldman, J.W.; Senior, A.K.; Cooper, A.B. (1999). Long Bay Sedimentation Study: Stage I (Sediment Generation) and Stage II (Sediment Fate). NIWA Client Report NS000209

Green, M.O.; Oldman, J.W. (1999). Deposition of flood-borne sediment in Okura estuary. NIWA Client Report: ARC90242/2.

Gorman, R.M.; Bryan, K.R.; Laing, A.K. (2003). Wave hindcast for the New Zealand region: deep-water wave climate. *New Zealand Journal of Marine and Freshwater Research 37:* 589-612.

Hsu, S.A. (1986). Correction of land-based wind data for offshore applications: A further evaluation. *Journal of Physical Oceanography 16(2):* 390-394.

Laing, A.K.; Revell, M.J.; Brenstrum, E. (1997). "ERS scatterometer observations of airflow around mountainous islands." Presented at the Proceedings of the 3rd ERS Symposium on Space at the Service of our Environment, Florence, Italy.

Oldman, J.W.; Black K.P. (1997). Mahurangi estuary numerical modelling. NIWA Client Report: ARC60208/1

Oldman, J. W.; Swales, A. (1999). Mangemangeroa estuary numerical modelling and sedimentation. NIWA Client Report: ARC70224.

Oldman, J.W.; Senior, A.. (2000) Wilson Bay Marine Farm Dispersal Modelling NIWA Client Report: EVW01218

Stephens, S.A.; Liefting, H.C.C. (2003). Current and wave measurements in the Te Tapuwae O Rongokako Marine Reserve during September-October 2003. *NIWA consulting report to the Department of Conservation, No. HAM2003-138.* 18 p.

Taylor, D.; Schiel, D.; Stevens, C.L. (2004). "Fluid dynamics and sub-millimetre physics in the ecology of a rocky reef. boundary layers and early life stages of habitat-forming algae." Presented at the New Zealand Marine Sciences Society Annual Conference, Dunedin, 6-8 July 2004.

Vance, R. R. (1973). On reproductive strategies in marine benthic invertebrates. *American Naturalist 107:* 339-352.

Walters, R.A.; Goring, D.G.; Bell, R.G. (2001). Ocean tides around New Zealand. *New Zealand Journal of Marine and Freshwater Research 35:* 567-579.

Young, I.R. (ed.) (1999). Wind generated ocean waves. *Ocean Engineering Series.* Elsevier, Amsterdam. 288 p.

Continue to next file: MCU10b.pdf